

## Electronic supporting information

### Experimental details

#### Materials

Oxidised carbon nanocones (ox-CNCs) were supplied by n-TEC ([www.n-tec.no](http://www.n-tec.no)), and they feature an approximate composition of 20% cones, 70% disks and 10% amorphous carbon. Titanium n-butoxide (97%), mercaptoundecanoic acid (MUA) and  $K_2PdCl_4$  were purchased by Sigma-Aldrich. Ethanol was of absolute grade ( $\geq 99.8\%$ ) and was purchased by Fluka.

#### Synthesis

A given amount of ox-CNCs (chosen in order to have a 20 wt% relative to the theoretical final composition) were dispersed in ethanol (reaching 2 mg/mL concentration) by sonication (30 minutes). Meanwhile, the Pd@TiO<sub>2</sub> precursors were assembled by slowly adding a THF solution of previously prepared mercaptoundecanoic acid-capped Pd nanoparticles to a EtOH solution of Ti(n-OBu)<sub>4</sub>, as reported elsewhere.<sup>1,2</sup> We chose a Pd loading as to have a final nominal 1% wt in the final hybrid. The as-prepared Pd@TiO<sub>2</sub> precursors were then added to the CNCs dispersion and the mixture sonicated for 30 minutes. After this time, a 10% solution of H<sub>2</sub>O in EtOH (Ti(n-OBu)<sub>4</sub>/H<sub>2</sub>O molar ratio: 1/100) was added dropwise, followed by 30 minutes of sonication. The solid was filtered through a 0.45 μm PTFE filter and washed with ethanol. The product was recovered and dried at 85°C overnight (**ox-CNCs/Pd@TiO<sub>2</sub>**). Part of the product was subjected to calcination at 350°C for 5 hrs, and labelled **ox-CNCs/Pd@TiO<sub>2</sub>-350**. As a comparison, two catalysts not featuring either CNCs, labelled **Pd@TiO<sub>2</sub>-350**, or Pd, labelled **CNCs/TiO<sub>2</sub>-350** were also prepared using the same synthetic approach but in absence of the respective component.

#### Characterisation

TEM measurements were performed on a TEM Philips EM208, using an acceleration voltage of 100 kV. Samples were prepared by drop casting the dispersed particles onto a TEM grid (200 mesh, copper, carbon only). High resolution TEM (HRTEM) were acquired on a JEOL 2200FS microscope operating at 200 kV, equipped with an Energy Dispersive Spectrometer (EDS), in-column energy (Omega) filter, and High-Angle Annular Dark-Field (HAADF) detector.

Thermogravimetric analysis (TGA) was performed on TGA Q500 (TA Instruments) under air, equilibrating at 100°C, and following a ramp of 10 °C min<sup>-1</sup> up to 800 °C.

Raman spectra were recorded on a inVia Renishaw microspectrometer equipped with a Nd:YAG laser using an excitation wavelength of 532 nm. Preparation of the samples was carried out via drop casting the dispersed particles onto silicon wafers, which were then analysed. For each sample, 5 points were recorded and averaged.

X-ray Diffraction (XRD) patterns were collected on a Philips X'Pert diffractometer using a monochromatized Cu K $\alpha$  ( $\lambda = 0.154$  nm) X-ray source in the range  $20^\circ < 2\theta < 100^\circ$ . The mean crystallite sizes of the TiO<sub>2</sub> were calculated by applying the Scherrer equation to the anatase (101) reflection.

N<sub>2</sub> physisorption at the liquid nitrogen temperature was collected using a Micromeritics ASAP 2020 analyser. Before analysis, the samples were degassed at 150 °C for at least 12h at a pressure lower than 10  $\mu$ mHg. The specific surface area of the samples was calculated applying the BET method or the Langmuir equation, depending on the shape of N<sub>2</sub> physisorption isotherms. Pore size distributions were calculated applying the BJH method to the adsorption branch of the isotherms.

Fourier Transform Infrared spectroscopy (FTIR) was measured in a System 2000 - Perkin Elmer spectrometer in an optical range of 370-4000 cm<sup>-1</sup> at a resolution of 4 cm<sup>-1</sup>.

UV spectra were acquired on a UV-Vis spectrophotometer (Shimadzu UV-2450). Samples were dispersed in ethanol in concentration 0.1 mg/mL in a quartz cuvette and spectra run between 200-900 nm.

### Photocatalytic experiments

For the UV experiments, the H<sub>2</sub> evolution was evaluated using a 250 mL Pyrex discontinuous batch reactor with an external cooling jacket. A nominal 10 mg of catalyst was loaded in the reactor, dispersed by sonication for 30 minutes in 60 mL of a water/ethanol mixture (1/1 by volume). The system was purged with Ar for 30 min to remove the air before switching on the lamp. All experiments were carried out at 20 °C, and 15 mL min<sup>-1</sup> of Ar were passed through the solution to transport the gaseous/volatile products to a GC for quantitative analysis. A 125 W medium pressure mercury lamp (Helios Italquartz) with Pyrex walls was used for UV-vis excitation. Gaseous products were analyzed by GC analysis using a thermal conductivity detector (TCD) for H<sub>2</sub> quantification and a methanator followed by a flame ionization detector (FID) for the detection of the volatile organic compounds.

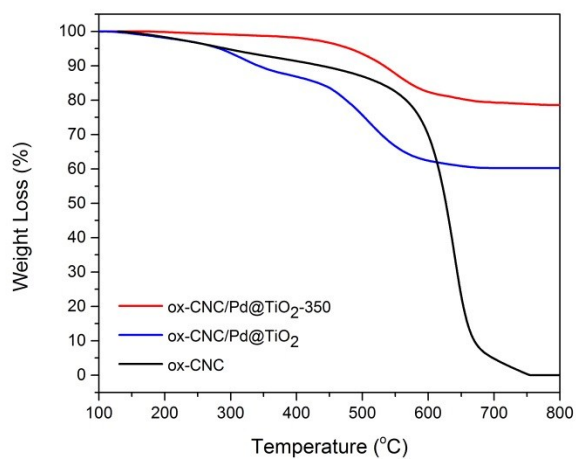
For the solar-simulated experiments, photocatalytic H<sub>2</sub> production was studied using a Teflon-lined flow-photoreactor irradiated with a Lot-Oriel Solar Simulator equipped with a 150 W Xe lamp and an Atmospheric Edge Filter with a cut-off at 300 nm. <sup>3</sup>

Quantum efficiency (QE) was calculated with equation (1):

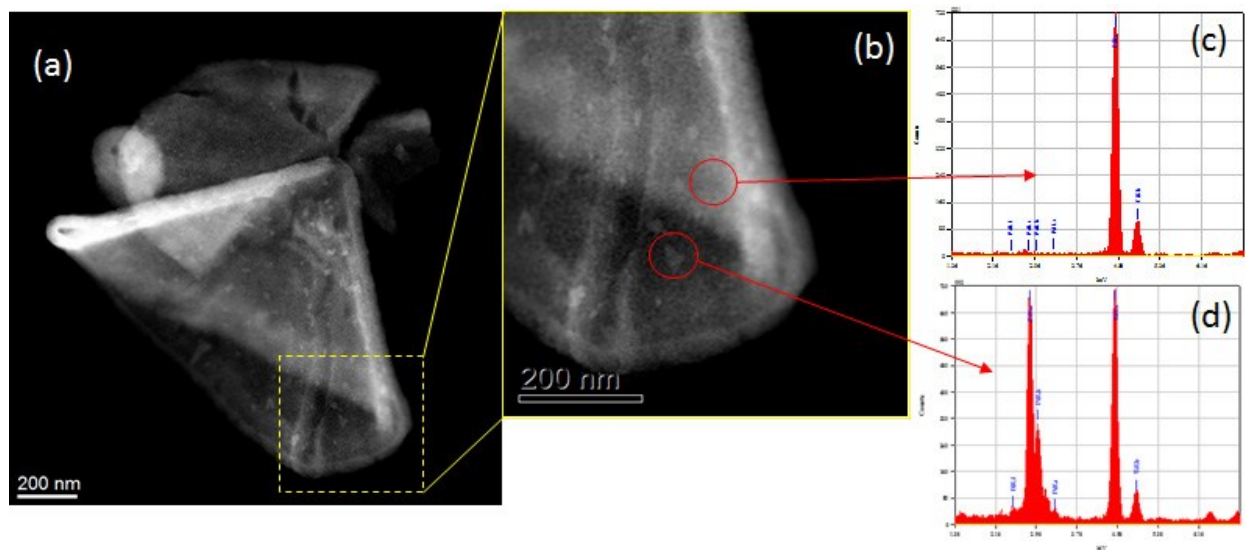
$$QE = 2 \cdot \text{mol H}_2 / \text{absorbed photons} \quad (1)$$

irradiating the sample with a 4 W Hg Penray.

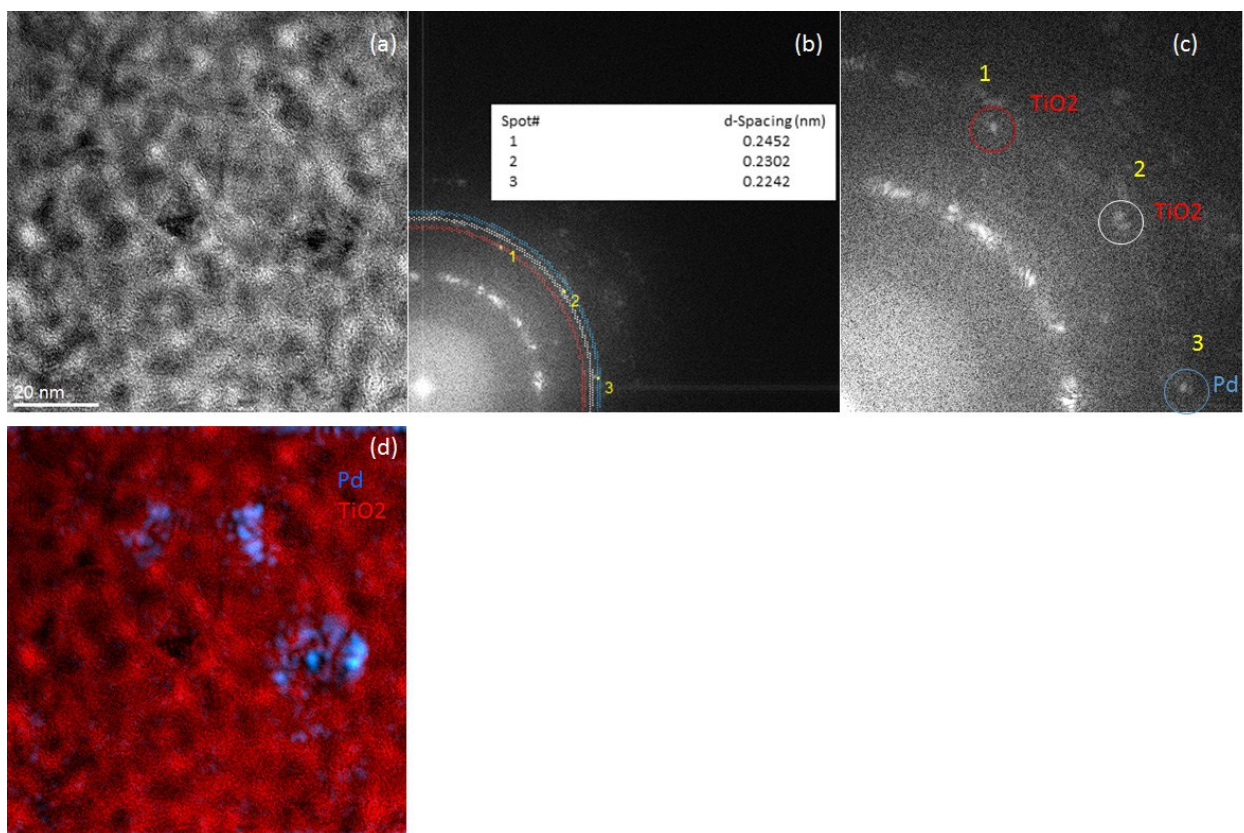
Recyclability of the best performing catalyst (**CNCs/Pd@TiO<sub>2</sub>-350**) was evaluated by using the recovered catalyst after a 20 h catalytic experiment for three catalytic cycles, and reporting the total H<sub>2</sub> productivity over time normalized by the catalyst surface area.



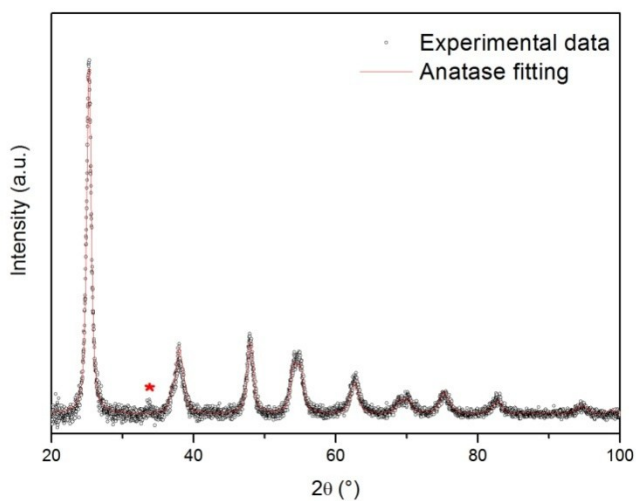
S1. Thermogravimetric analysis (TGA) analysis of **ox-CNCs/Pd@TiO<sub>2</sub>-350**, **ox-CNCs/Pd@TiO<sub>2</sub>** and **ox-CNCs**.



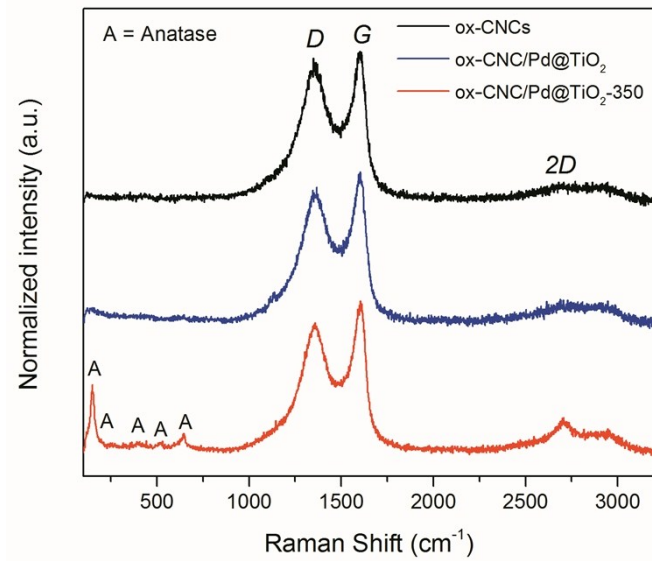
S2. a) HAADF image and zoom-in (b) of a **CNCs/Pd@TiO<sub>2</sub>-350** typical structure. c, d) EDX spectra of regions without and with bright features, respectively.



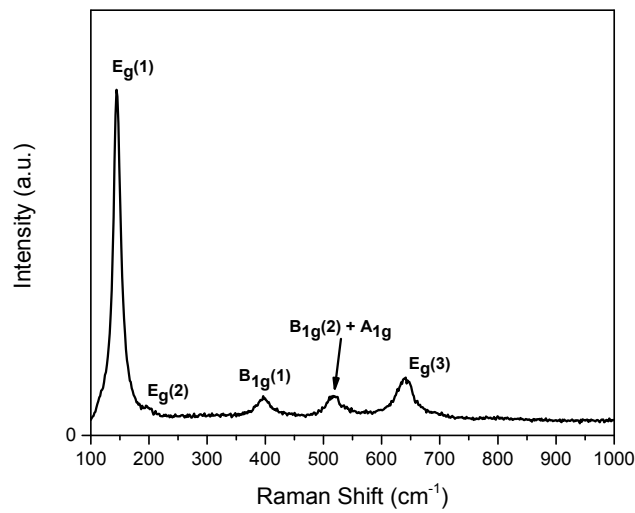
S3. a) HRTEM image of **CNCs/Pd@TiO<sub>2</sub>-350**; b, c) corresponding FFT showing spots corresponding to the TiO<sub>2</sub> anatase phase and Pd; d) color map displaying the inverse FFT generated by selecting the diffraction spots of TiO<sub>2</sub> (red) and Pd (blue).



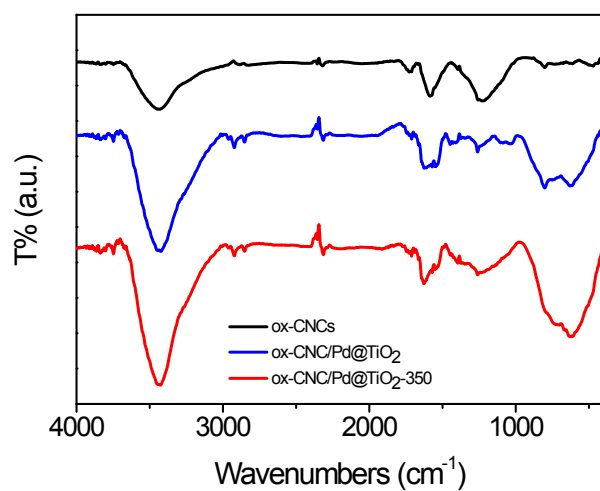
S4. Experimental XRD of **CNCs/Pd@TiO<sub>2</sub>-350** and fitting with the spectrum of anatase. Peak with asterisk in XRD = FeTi<sub>2</sub>O<sub>4</sub> impurity.



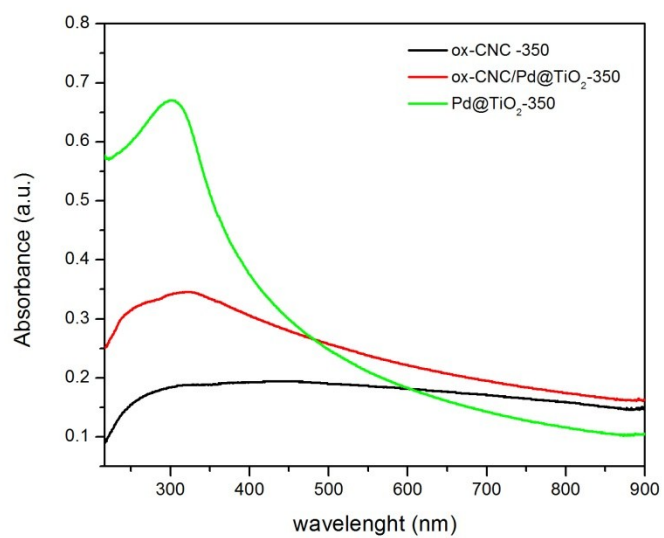
S5. Raman analysis of **ox-CNCs**, **ox-CNCs/Pd@TiO<sub>2</sub>** and **ox-CNCs/Pd@TiO<sub>2</sub>-350**.



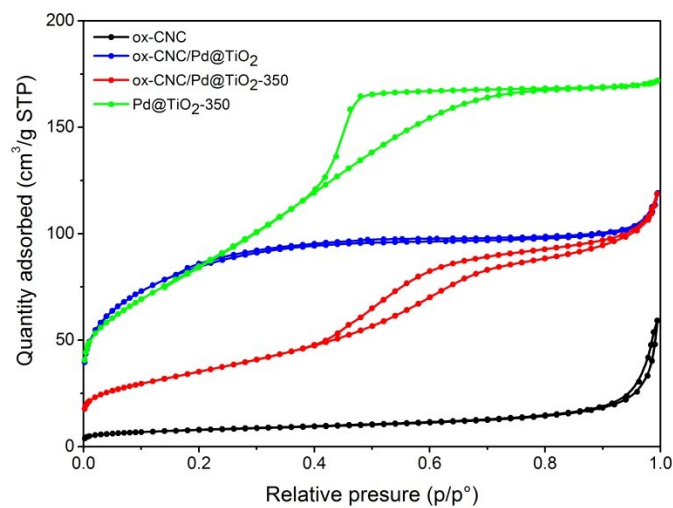
S6. Expanded window between 100 and 1000  $\text{cm}^{-1}$  of the Raman spectrum of **CNCs/Pd@TiO<sub>2</sub>-350** showing the fingerprint peak pattern of anatase TiO<sub>2</sub>.



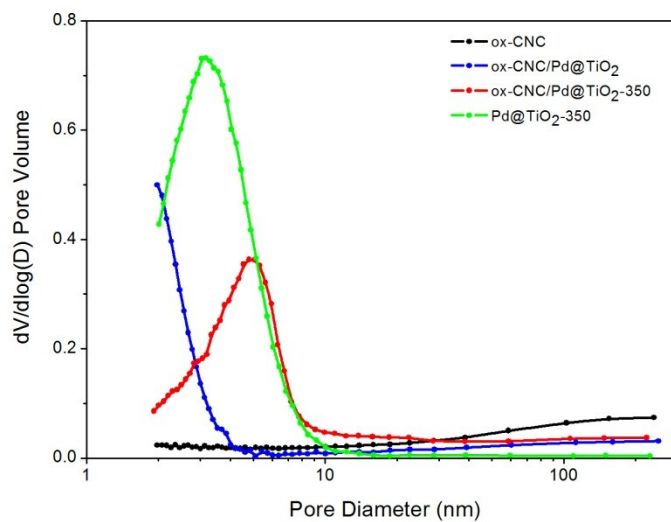
S7. FTIR analysis of **ox-CNCs**, **ox-CNCs/Pd@TiO<sub>2</sub>** and **ox-CNCs/Pd@TiO<sub>2</sub>-350**.



S8. UV-Vis spectrum of **CNC-350**, **Pd@TiO<sub>2</sub>-350** and **ox-CNCs/Pd@TiO<sub>2</sub>-350**



S9. N<sub>2</sub> physisorption isotherms of **ox-CNCs**, **ox-CNCs/Pd@TiO<sub>2</sub>**, **ox-CNCs/Pd@TiO<sub>2</sub>-350** and **Pd@TiO<sub>2</sub>-350**.



S10. BJH pore size distributions calculated on the adsorption branches for **ox-CNCs**, **ox-CNCs/Pd@TiO<sub>2</sub>**, **ox-CNCs/Pd@TiO<sub>2</sub>-350** and **Pd@TiO<sub>2</sub>-350**.

**Table S1. Summary of results from analysis of the N<sub>2</sub> physisorption isotherms of the investigated samples.**

Sample	Pd@TiO <sub>2</sub> -350	Ox-CNCs	Ox-CNCs/Pd@TiO <sub>2</sub> Fresh	Ox-CNCs/ Pd@TiO <sub>2</sub> -350
Type of isotherm <sup>a</sup>	IV	II	I	IV
Specific Surface Area (m <sup>2</sup> /g)	323	25 <sup>b</sup>	248 <sup>c</sup>	126 <sup>b</sup>
Cumulative Pore Volume (mL/g)	0.295	0.089 <sup>d</sup>	0.112 <sup>e</sup>	0.192 <sup>d</sup>
D <sub>max</sub> (nm) <sup>f</sup>	3.2	> 200	< 2	4.9

<sup>a</sup> accordingly to IUPAC recommendation.<sup>4</sup>

<sup>b</sup> Calculated using the BET equation.

<sup>c</sup> Calculated using the Langmuir equation.

<sup>d</sup> Calculated from the BJH analysis of the adsorption branch of the N<sub>2</sub> physisorption isotherms.

<sup>e</sup> Calculated from the adsorbed volume at p/p° = 0.90, in agreement with what published.<sup>5</sup>

<sup>f</sup> Maximum of the pore size distribution obtained applying the BJH analysis to the adsorption branch of the N<sub>2</sub> physisorption isotherms, as reported in Fig S10.

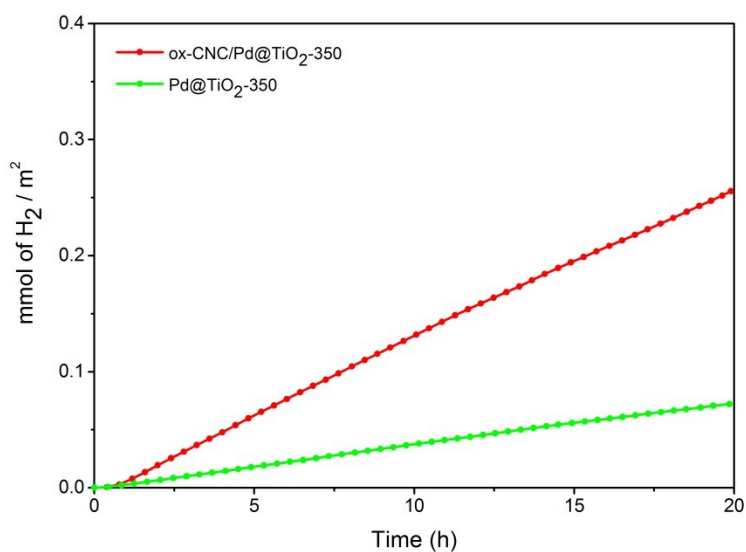


Fig S11. H<sub>2</sub> production over time by **ox-CNCs/Pd@TiO<sub>2</sub>-350** and **Pd@TiO<sub>2</sub>-350** normalised by the initial surface area of the catalysts under UV-Vis illumination. No activity was detected with **ox-CNCs/Pd@TiO<sub>2</sub>** under the catalytic conditions.

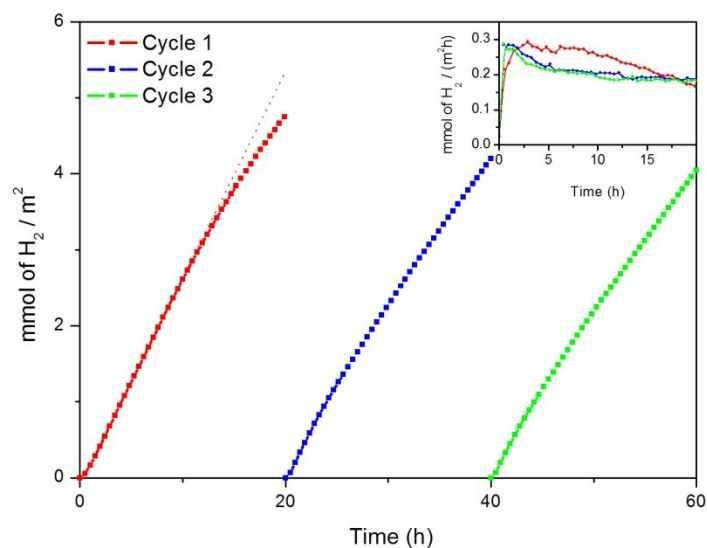


Fig S12. Catalytic activity (normalised by the catalysts initial surface area) of **ox-CNCs/Pd@TiO<sub>2</sub>-350** over three different cycles. The red dotted line represents the theoretical activity if no deactivation processes were in place and it can be used as guide.

**Table S2. Comparison with the performance of some recent catalytic systems containing carbon supports and integrated metal phases.**

Entry	Carbon Support	Metal phase	Maximum Rate of H <sub>2</sub> evolution (mmol·g <sup>-1</sup> ·h <sup>-1</sup> )	Hole scavenger	Quantum efficiency	Power of irradiating lamp	Reference
1.	Ox-MWCNT	Pt/TiO <sub>2</sub>	40	Methanol	Not reported	200W (240-500 nm range)	6
2.	Ox-MWCNTs	Pt/TiO <sub>2</sub>	10	Methanol	Not reported	125W (λ>365)	7
3.	GO	TiO <sub>2</sub>	0.4	Methanol	Not reported	300W (λ>320nm)	8
4.	GO	Cu/TiO <sub>2</sub>	19	Methanol	Not reported	300W (λ>365)	9
5.	g-C <sub>3</sub> N <sub>4</sub>	Pt	0.15	Triethanolamine	Not reported	300W (λ>420)	10
6.	Ox-CNTs	TiO <sub>2</sub>	2	Glycerol	Not reported	Not specified	11
7.	Ox-MWCNTs	Pt/TiO <sub>2</sub>	8	Triethanolamine	Not reported	250W (λ>320)	12
8.	GO	TiO <sub>2</sub>	0.7	Methanol	QE = 3.1%	350W (λ>320)	13
9.	GO	Pt/CdS	55	Lactic Acid	QE = 22%	350W (λ>420)	14
10.	C <sub>60</sub> -SWCNTs	TiO <sub>2</sub>	3.2	Triethanolamine	Not reported	300W (λ>320)	15
11.	GO	Pt/Sr <sub>2</sub> Ta <sub>2</sub> O <sub>7-x</sub> N <sub>x</sub>	3	Methanol	QE = 6.5%	300W (λ>420)	16
12.	MWCNTs	Pt/Ta <sub>2</sub> O <sub>5</sub>	32	Methanol	Not reported	450W (λ>365)	17
13.	RGO	TiO <sub>2</sub>	1	Ethanol	Not reported	300W (λ>320)	18
<b>14.</b>	<b>CNCs</b>	<b>Pd/TiO<sub>2</sub></b>	<b>37</b>	<b>Ethanol</b>	<b>QE = 12%</b>	<b>125W (λ&gt;365)</b>	<b>This work</b>

GO = graphene oxide; RGO = Reduced graphene oxide

<sup>1</sup> a) M. Cargnello, J. J. Delgado Jaén, J. C. Hernández Garrido, K. Bakhmutsky, T. Montini, J. J. Calvino Gámez, R. J. Gorte, P. Fornasiero, *Science* 2012, **337**, 713-717; b) K. Bakhmutsky, N. L. Wieder, M. Cargnello, B. Galloway P. Fornasiero, Raymond J. Gorte, *ChemSusChem* 2012, **5**, 140-148.

<sup>2</sup> K. Bakhmutsky, N. L. Wieder, M. Cargnello, B. Galloway P. Fornasiero, Raymond J. Gorte, *ChemSusChem* 2012, **5**, 140-148.

<sup>3</sup> G. Carraro, C. Maccato, A. Gasparotto, T. Montini, S. Turner, O. I. Lebedev, V. Gombac, G. Adami, G. Van

- 
- Tendeloo, D. Barreca, P. Fornasiero *Adv. Funct. Mater.* 2014, **24**, 372-378.
- <sup>4</sup> K. S. W. Sing, D. H. Everett, R. A. W. Haul, L. Moscou, R. A. Pierotti, J. Rouquerol, T. Siemieniewska, *Pure Appl Chem*, 1985, **57**, 603–619
- <sup>5</sup> Chapter 4 of Gregg & Sing, “Adsorption, Surface Area & Porosity”, Academic Press Inc. New York, 1981
- <sup>6</sup> A. Moya, A. Cherevan, S. Marchesan, P. Gebhardt, M. Prato, D. Eder, J. J. Vilatela *Appl Catal B: Environmental* 2015, **179**, 574–582
- <sup>7</sup> M. Cargnello, M. Grzelczak, B. Rodriguez-Gonzalez, Z. Syrgiannis, K. Bakhmutsky, V. La Parola, L. M. Liz-Marzan, R. J. Gorte, M. Prato, P. Fornasiero *J. Am. Chem. Soc.*, 2012, **134**, 11760
- <sup>8</sup> H. Kim, S. Kim, J.-K. Kang, W. Choi, *J. Catal* 2014, **309**, 49
- <sup>9</sup> X.-J. Lv, S.-X. Zhou, C. Zhang, H.-X. Chang, Y. Chen and W.-F. Fu, *J. Mater. Chem.*, 2012, **22**, 18542
- <sup>10</sup> K. Li, Z. Zeng, L. Yan, S.n Luo, X. Luo, M. Huo, Y. Guo, *App. Catal. B: Environmental* 2015, **165**, 428
- <sup>11</sup> M. MamathaKumari, D. Praveen Kumar, P. Haridoss, V. DurgaKumari, M.V. Shankar, *Int. J. Hydrogen Energ.* 2015, **40**, 1665.
- <sup>12</sup> K. Dai, T. Peng, D. Ke, B. Wei, *Nanotechnology* 2009, **20**, 125603.
- <sup>13</sup> Q. Xiang, J. Yu, M. Jaroniec, *Nanoscale* 2011, **3**, 3670
- <sup>14</sup> Q. Li, B. Guo, J. Yu, J. Ran, B. Zhang, H. Yan, J. Ru Gong, *J. Am. Chem. Soc.* 2011, **133**, 10878.
- <sup>15</sup> B. Chai, T. Peng, X. Zhang, J. Mao, K. Li, X. Zhang, *Dalton Trans.* 2013, **42**, 3402.
- <sup>16</sup> A. Mukherji, B. Seger, G. Qing Lu, L. Wang *ACS Nano*, 2011, **5**, 3483.
- <sup>17</sup> A. S. Cherevan, P. Gebhardt, C. J. Shearer, M. Matsukawa, K. Domen, D. Eder, *Energy Environ. Sci.*, 2014, **7**, 791
- <sup>18</sup> G. Nagaraju, K. Manjunath, S. Sarkar, E. Gunter, S. R. Teixeira, J. Dupont, *Int. J. Hydrogen Energ.* 2015, **40**, 12209.